ADVANCED HEALTHCARE MATERIALS

# Supporting Information

for *Adv. Healthcare Mater.*, DOI: 10.1002/adhm.201600222

# Subdermal Flexible Solar Cell Arrays for Powering Medical Electronic Implants

*Kwangsun Song, Jung Hyun Han, Taehoon Lim, Namyun Kim, Sungho Shin, Juho Kim, Hyuck Choo, Sungho Jeong, Yong-Chul Kim, Zhong Lin Wang, and Jongho Lee**

# Supporting Information

**Title**
Subdermal flexible solar cell arrays for powering medical electronic implants

*Author(s), and Corresponding Author(s)**
*Kwangsun Song, Jung Hyun Han, Taehoon Lim, Namyun Kim, Sungho Shin, Juho Kim, Hyuck Choo, Sungho Jeong, Yong-Chul Kim, Zhong Lin Wang and Jongho Lee**

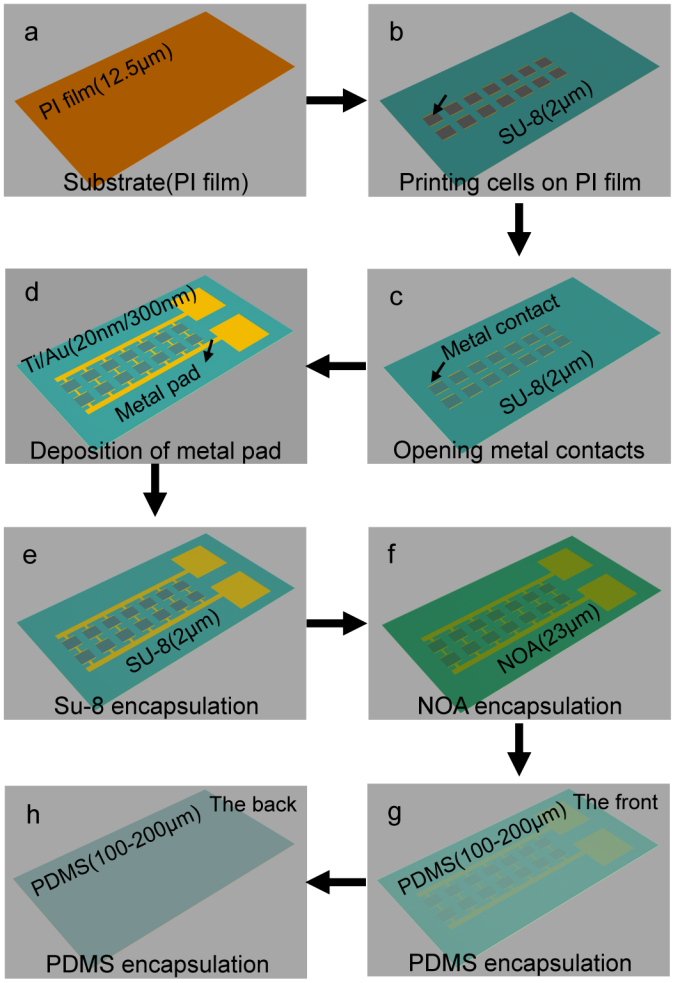


**Figure S1.** Schematic illustrations of the fabrication process for the implantable photovoltaic device. (a) Preparation of a polyimide film (thickness: 12.5 μm). (b) Fourteen microcells are transfer-printed on the PI film with aids of an adhesive layer (SU-8, thickness ~2 μm). (c) Via holes for top and bottom contacts by patterning SU-8. (d) Interconnection metals (Ti/Au) are deposited onto the top and bottom contacts. (e) SU-8 and (f) NOA layers are spun on the top layer. Layers of PDMS encapsulate the device on the (g) front and (g) back.

a

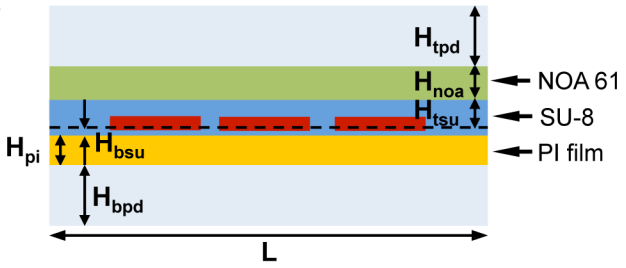


b

$E_{su}$=2 Gpa, $E_{pi}$=3.2 Gpa

$E_{noa}$=1 Gpa, $E_{pd}$=2 Mpa

$H_{pi}$=12.5 μm, $H_{tpd}$=$H_{bpd}$=100 μm,

$H_{tsu}$=10 μm, $H_{bsu}$=2 μm, $H_{noa}$=23 μm

L=7.5 mm, $L_{pi}$=$E_{pi}/E_{pd}$ × L,

$L_{su}$=$E_{su}/E_{pd}$ × L, $L_{noa}$=$E_{noa}/E_{pd}$ × L

$S_1$=$H_{bpd}/2$, $S_2$=$H_{pd}$+$H_{pi}/2$, $S_3$=$H_{pd}$+$H_{pi}$+($H_{bsu}$+$H_{tsu}$)/2

$S_4$=$H_{pd}$+$H_{pi}$+$H_{bsu}$+$H_{tsu}$+$H_{noa}/2$

$S_5$=$H_{pd}$+$H_{pi}$+$H_{bsu}$+$H_{tsu}$+$H_{noa}$+$H_{tpd}/2$

$A_1$=L×$H_{tpd}$, $A_2$=$L_{pi}$×$H_{pi}$, $A_3$=$L_{su}$×$H_{su}$,

$A_4$=$L_{noa}$ ×$H_{noa}$, $A_5$=$L_{tpd}$×$H_{tpd}$

$S_{neutral\ plane}$=$\sum S_iA_i/\sum A_i$,

$S_{neutral\ plane}$

=($S_1A_1$+$S_2A_2$+$S_3A_3$+$S_4A_4$+$S_5A_5$)/($A_1$+$A_2$+$A_3$+$A_4$+$A_5$)

$S_{neutral\ plane}$≈117.5 μm(center of microcells)

**Figure S2.** (a) The cross-sectional view of the IPV device. The inorganic solar materials (red) are located in mechanically neutral plane. (b) Dimensions and calculation of the neutral plane.

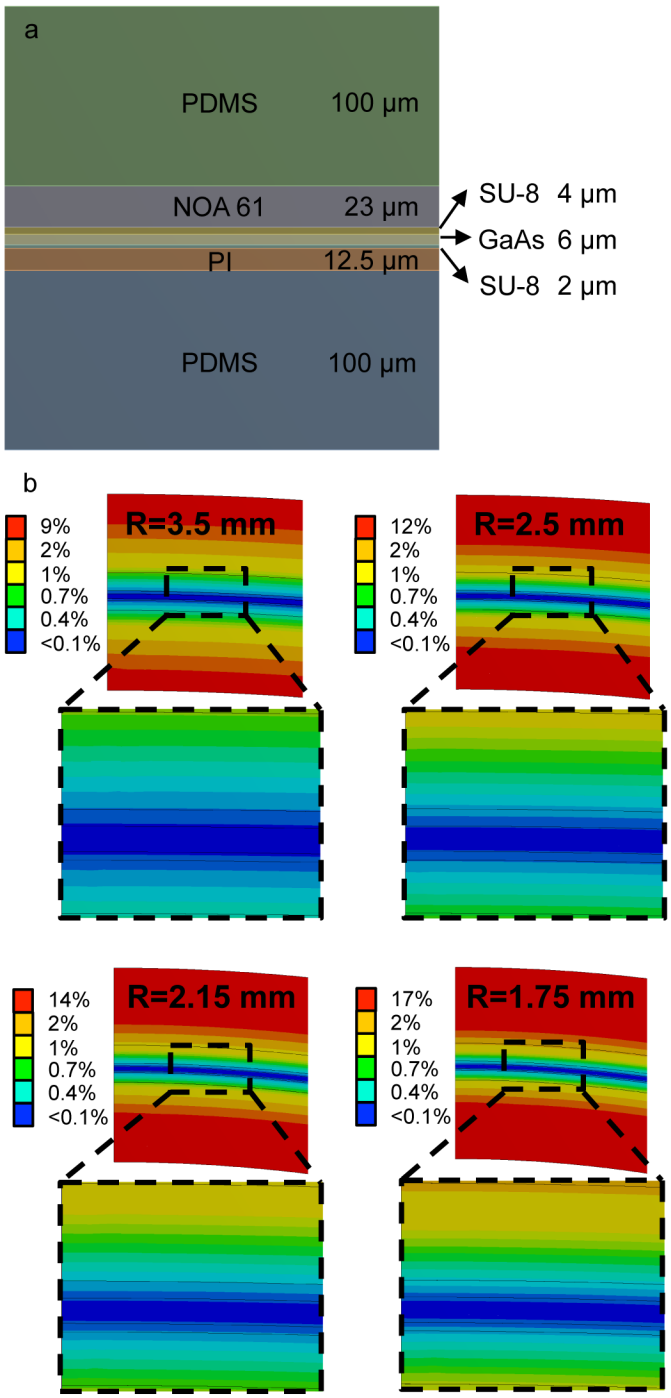


**Figure S3.** (a) Dimensions used in finite element method (FEM) analysis. (b) FEM results of the IPV devices bent with the radii of 3.5 mm, 2.5 mm, 2.15 mm and 1.75 mm. The strains in the solar microcells are minimal < 0.1% and < 0.3% with radii of curvature of ~3.5 mm and 1.75 mm, respectively.

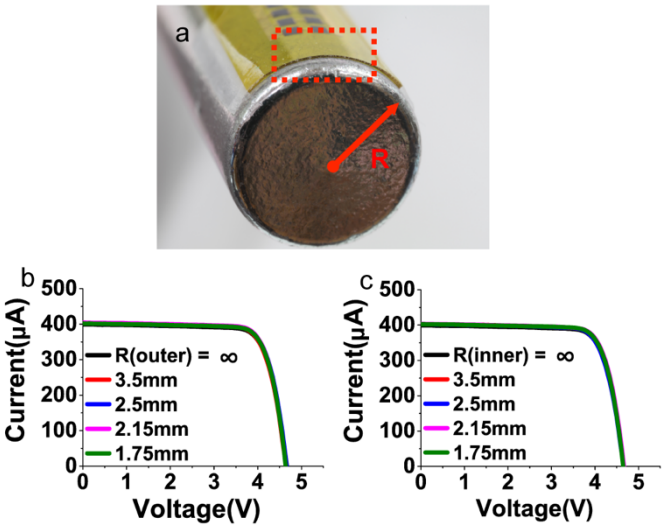


**Figure S4.** (a) Optical image of the IPV device on a cylinder (radius of curvature : 4 mm). (b)-(c) Current-voltage characteristics of the IPV device after bending and unbending on cylinders whose radii of curvature of 3.5 mm, 2.5 mm, 2.15 mm and 1.75 mm in (b) the outer and (c) inner directions.

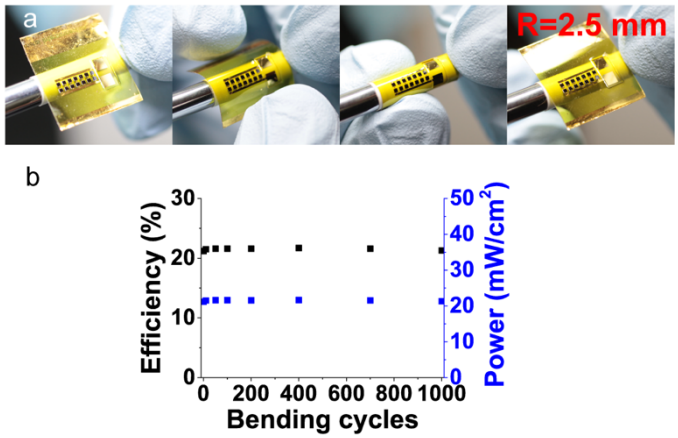


**Figure S5.** (a) Optical image of cycling tests on a cylinder with a radius of 2.5 mm. (b) Measurement results of the tests. There is not noticeable degradation of the efficiency and power density even after 1000 cycles.

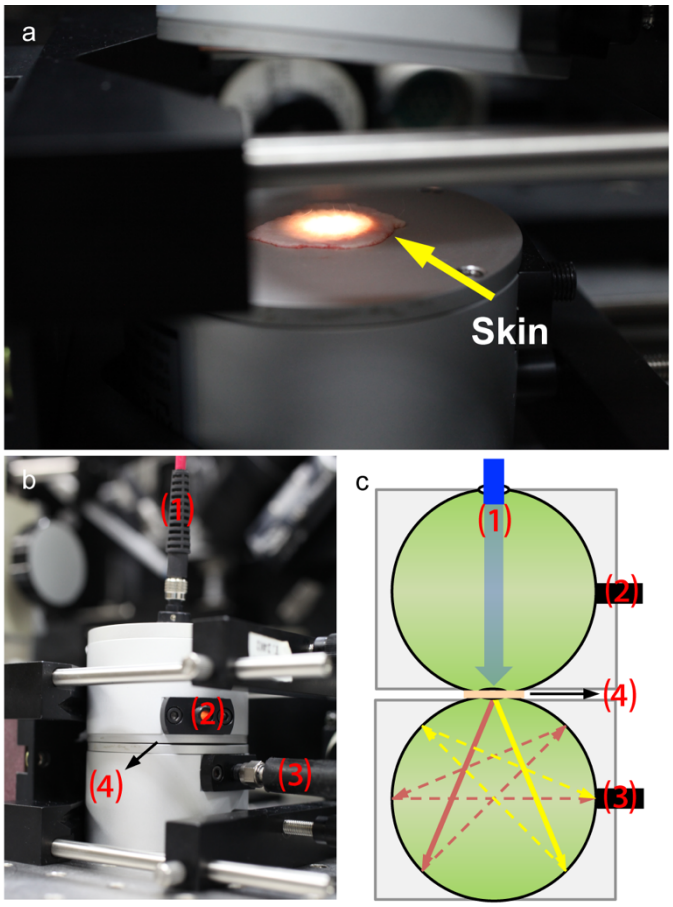


**Figure S6.** (a) Optical image of the hairless mouse skin mounted on a lower integrating sphere within 10 min after isolating from the mouse. (b) Optical image and (c) schematic illustration of the optical measurement system consisting of a light source, a pair of double-integrating spheres and detectors. Scattered light reflected on the skin or transmitted through skin is collected in the detectors.

$$J_{im,GaInP} = q\int_{400}^{900} T(\lambda)\Phi(\lambda)EQE(\lambda)d\lambda$$
$$= 5q\sum_{n=0}^{99} T(400 + 5n)\Phi(400 + 5n)EQE(400 + 5n)$$
$$J_{im,GaAs} = q\int_{400}^{900} T(\lambda)\Phi(\lambda)EQE(\lambda)d\lambda$$
$$= 5q\sum_{n=0}^{99} T(400 + 5n)\Phi(400 + 5n)EQE(400 + 5n)$$
$$J_{calc} = \alpha\min(J_{im,GaInP}, J_{im,GaAs})$$

q = Elementary charge [C]=1.6021765 × $10^{-19}$ C

T = Transmittance of skin

ϕ = Photon flux [$cm^{-2}$ $s^{-1}nm^{-1}$]

EQE = External quntum efficiency

J = Current density [$mA/cm^2$]

α = Constant to adjust current for different bare skin

**Figure S7.** Calculations of the current densities based on the transmittance of the mouse skin, photon flux of the irradiation[62] and external quantum efficiency (EQE) of the solar microcells.

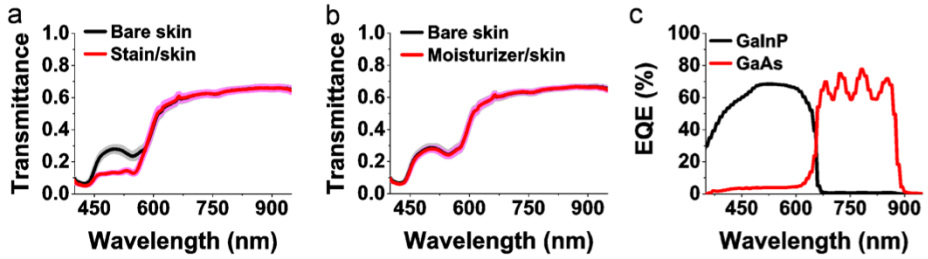


**Figure S8.** Transmittance (mean ± SEM, n = 7) measurements of bare skins (black line) and the skins (red line) covered with (a) cheek-and-lip stain, (b) moisturizer. (c) Quantum efficiency of the solar microcells.

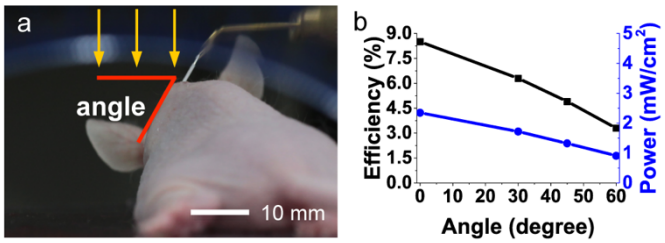


**Figure S9.** (a) Image of the hairless mouse with the IPV device illuminated at a tilted angle. (b) Conversion efficiency and electric power density when the implanted IPV device tilted by 0°, 30°, 45° and 60° from the perpendicular plane to the incident light. At relatively high angle (~60°), the subdermal IPV device still generate 38% of power (0.9 mW/cm$^2$) compared the one (2.35 mW/cm$^2$) generated without tilting.

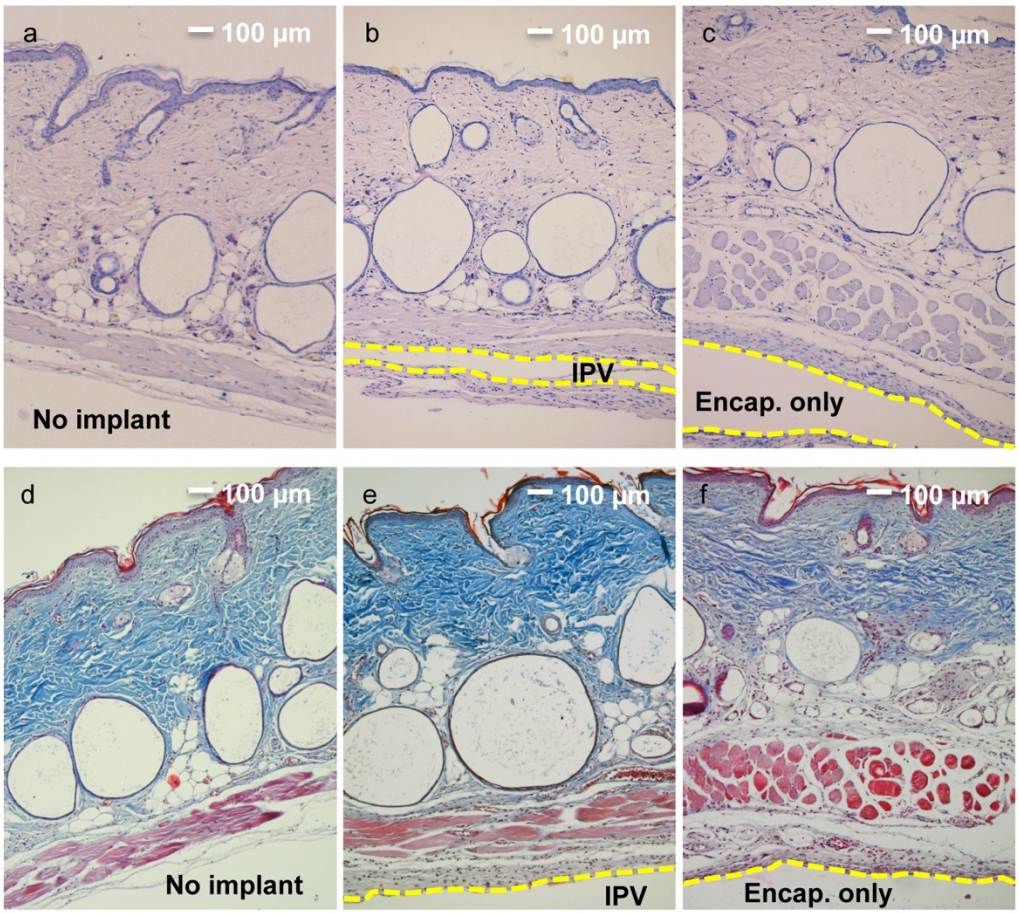


**Figure S10.** (a-c) Histological images of the hairless mouse skin tissues, stained with hematoxylin and eosin (H&E), with (a) no implant, (b) encapsulation layer only and (c) the IPV device after 4 weeks of implantation. (d-f) Histological images of the hairless mouse skin tissues, stained with Accustain trichrome stain (Masson) kit (Sigma), with (d) no implant, (e) encapsulation layer only and (f) the IPV device after 4 weeks of implantation.

a

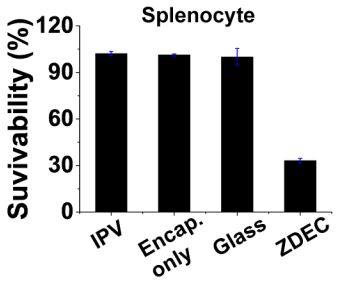


**Figure S11.** Viability of splenocytes, immune cells obtained from spleen of a hairless mouse, when exposed directly to the IPV devices, encapsulation layers only, glass slides, ZDEC-PU films for 24 hours. Survivability of the immune cells for the IPV device and encapsulation layers only is similar with the control (glass). However, survivability with ZDEC-PU films decreases down to ~30%.

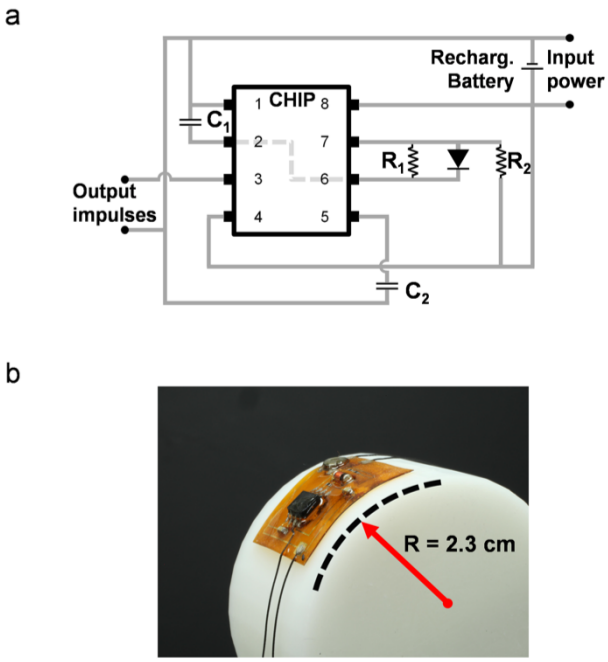


**Figure S12.** (a) Electric circuit diagram of the subdermally implantable flexible pacemaker ($R_1$ = 4.7 MΩ, $R_2$ = 23.8 kΩ, $C_1$ = 100 nF, $C_2$ = 10 nF). (b) Optical image of the flexible pacemaker bent on a cylinder with a radius of 2.3 cm.

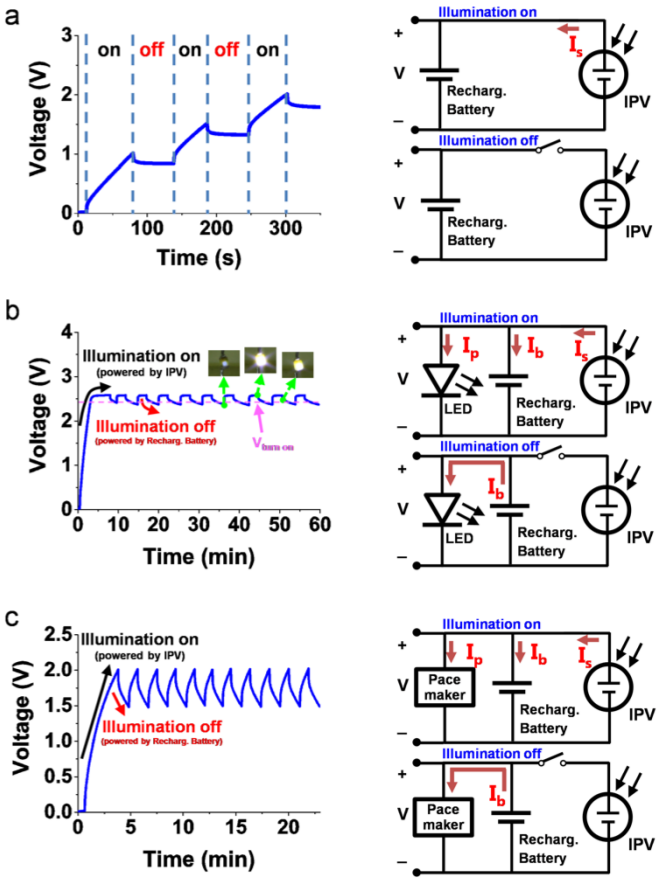


**Figure S13.** (a) Characteristics of charging and holding of the rechargeable battery by the IPV device under skin (left) and the equivalent circuit diagrams (right) when the illumination is repetitively on/off. Voltage drop (ΔV = 0.15 V) at illumination off is caused by the internal resistance in the battery. In the design, the current flowing back through the IPV device while illumination off is small because the shunt resistance (0.7-2 MΩ) of the solar microcell is very large and turn-on voltage (~4 V) of two diodes in series is greater than the output voltage (3.3 V) of the battery. For improved pacemakers, an additional power management system should be able to shut off any leakage current. (b-c) Charging/loading characteristics (left) and the equivalent circuit diagrams (right) of the rechargeable battery and IPV device integrated with (b) a LED or (c) subdermally implantable pacemaker.

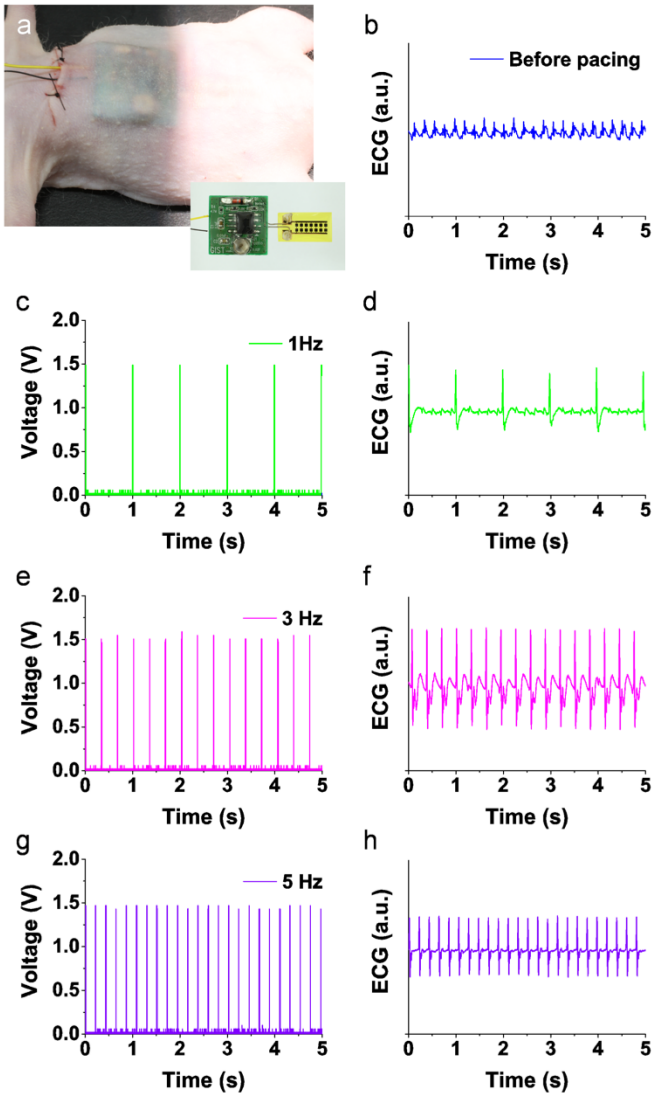


**Figure S14.** Self-powered pacemaker regulating the heart rate in different frequencies. (a) The subdermally implanted self-powered pacemaker powered by the IPV device and battery recharged by the IPV device. Inset: optical image of the self-powered pacemaker integrated with the IPV device. (b) ECG signal (~5 Hz) of the hairless mouse within ~5 min after opening the thoracic cage. (c) Impulses generated from the self-powered pacemaker and (d) regulated heart rate of the mouse in ~1 Hz (~10 min after opening of thoracic cage), (e-f) 3 Hz (~30 min after opening of thoracic cage) and (g-h) ~5 Hz (~40 min after opening of thoracic cage).

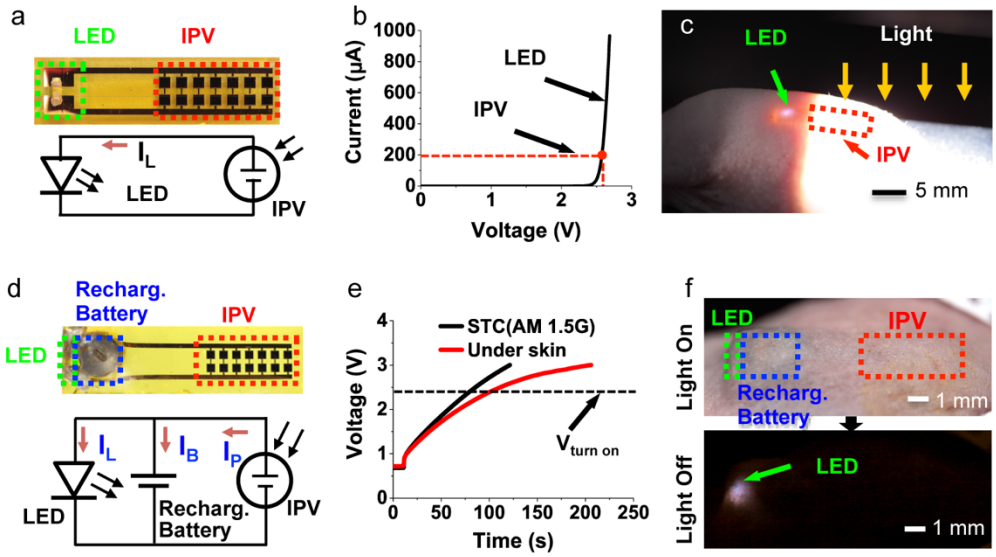


**Figure S15.** Fully implantable electronics integrated with the IPV devices. (a) An electronic device (LED) integrated with the IPV device and its equivalent circuit. (b) Current-voltage characteristics of the LED. Open-circuit voltage (~4.5 V) of the IPV device is high enough to turn on the LED ($V_{turn\text{-}on}$ = 2.4 V). (c) An image of LED light in a live hairless mouse when the IPV device is illuminated under AM1.5G. (d) An optical image of the integrated IPV device containing a rechargeable battery and the LED, and its equivalent circuit. The current ($I_P$) generated by the IPV device turns on the LED ($I_L$) and recharges the battery ($I_B$). (e) Charging time of the battery by the IPV device in a standard testing condition (STC, AM1.5G, black solid line) and under the skin of a live mouse (red solid line). (f) The integrated IPV device fully implanted under the mouse skin. With illumination on, the IPV device power the LED and stores energy to the rechargeable battery. With illumination off, the battery powers the LED with the stored energy.

**Charging a pacemaker battery with the IPVs**

Implantable photovoltaics
- Conversion efficiency : 8.2%
- Current : 160 μA

Pacemaker: Adapta ADDRS1, Medtronics
- Capacity : 830 mAh (Sigma 213 lithium-iodine)
- Longevity : 8 years (DDDR or DDD 50% mode)
- Rate and pulse width: 60 ppm, 0.4 ms
- Lead impledance: 1000 Ω
- Charging efficiency : 85%

Daily power consumption
= 830 mAh/(8×365 day) = 0.28425 mAh/day
Charging time for power consumption
= 0.28425 mAh/(0.16 mA×0.85) ≈ 2 hr 6 min

**Figure S16.** Calculation of charging time of a rechargeable battery whose capacity is same as a battery used in a pacemaker. The calculation indicates that recharging for 2 hr and 6 min provides enough energy to run a pacemaker for a day.

a

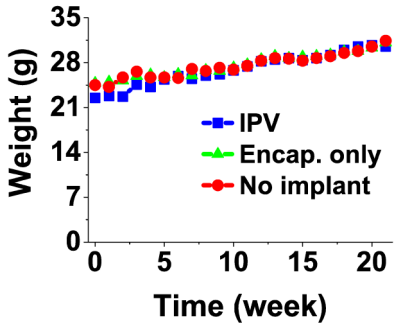


**Figure S17.** Weight measurements of the hairless mice with no implant (red), the IPV device (blue) and encapsulation only (green) for 21 weeks after implantation. The hairless mouse with the IPV device did not lose weight, similar with mice with no implant and encapsulation only.

| Additional layer | Ingredients | Volume or thickness | Efficiency |
|---|---|---|---|
| Sunscreen | bis-ethylhexyloxyphenol methoxyphenyltriazine, titanium dioxide, ethylhexylmethoxycinnamate, etc. | ~9 mg/cm$^2$ | 7.5% |
| Moisturizer | glycerin, butylene glycol, dipropylene glycol, etc. | ~13 mg/cm$^2$ | 7.8% |
| Cheek-and-lip stain | ethylhexyl stearate, butylene glycol, pentylene glycol, etc. | ~5 mg/cm$^2$ | 6.1% |
| Hydrocolloid bandage | carboxymethyl cellulose, pectin, gelatin, etc. | ~0.53 mm | 6.1% |

**Table S1.** Efficiencies of the IPV implanted under skin covered with additional layers such as sunscreen, moisturizer, cheek-and-lip stain, hydrocolloid bandage. Conversion efficiency of the IPV devices under the skin covered by sunscreen ($\eta$ = 7.5%, IOPE UV shield sun protector SPF 50+/PA+++$^{TM}$, Amorepacific) or moisturizer ($\eta$ = 7.8%, Shea butter steam cream moist$^{TM}$, Nature republic) is comparable to that ($\eta$ = 7.8%) with the bare skin only. Sunscreens usually designed to block ultraviolet (UV, wavelength: 280-400 nm)[49] affect minimally to transmittance of visible light that the IPV devices mostly absorb. Cheek-and-lip stain (Benefit cosmetics) or hydrocolloid bandage (thickness ~ 0.53 mm, Boryung) reduce conversion efficiency down to 6.1%.

**Video S1.** Regulated heart beat of a hairless mouse (SKH1 Hr$^{Hr}$) by the subdemally implanted self-powered flexible pacemakers.

**Video S2.** A hairless mouse (SKH1 Hr$^{Hr}$) with a subdermal IPV device.

**Video S3.** A fully implanted LEDs powered by the subdermal IPV device in a hairless mouse model (SKH1 Hr$^{Hr}$).

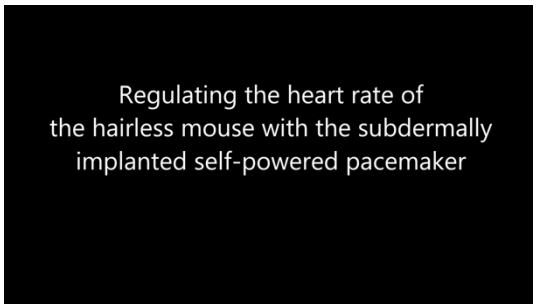
Regulating the heart rate of
the hairless mouse with the subdermally
implanted self-powered pacemaker

Video S1

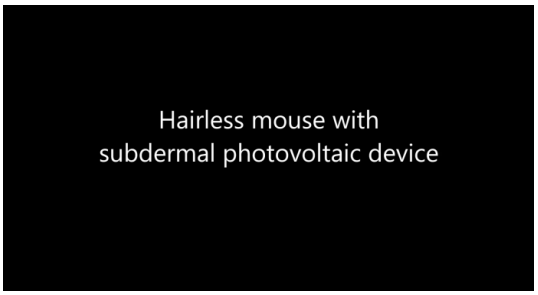


Video S2

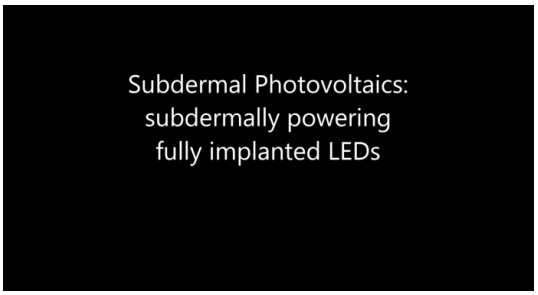
Subdermal Photovoltaics:
subdermally powering
fully implanted LEDs

Video S3